THE ASTRONOMICAL JOURNAL VOLUME 95, NUMBER 2 FEBRUARY 1988

NEAR-INFRARED STELLAR-OCCULTATION PREDICTIONS FOR URANUS AND NEPTUNE: 1987–1990

PHILIP D. NICHOLSON AND BRIAN A. MCLEOD
Department of Astronomy, Cornell University, Ithaca, New York 14853

GERARD GILMORE
Institute of Astronomy, Madingley Road, Cambridge CB3 0HA, England

MARC W. BUIE[a)]
Institute for Astronomy, University of Hawaii, Honolulu, Hawaii 96822

KEITH MATTHEWS
Palomar Observatory, California Institute of Technology, Pasadena, California 91125
Received 18 September 1987

ABSTRACT

Stellar-occultation predictions are presented for Uranus and Neptune covering the period 1987–1990, based on automated scans of *R* and *I* plates taken with the U.K. Schmidt Telescope in Australia. These scans have revealed many late-type or highly reddened stars suitable for stellar-occultation observations at λ 2.2 μm that were missed in previous searches of yellow-sensitive astrographic plates (Mink and Klemola 1985). Comparisons involving several hundred stars measured by Mink and Klemola (1985) indicate that the internal random errors in our stellar positions are $\lesssim 0.2''$, comparable to the precision reached using conventional astrographic methods. We have also obtained *JHK* photometry for many of the Neptune stars, which is used to establish an empirical $(I-K)$ vs $(R-I)$ calibration for the remaining occultation candidates, and thus provide estimates of their *K* magnitudes.

I. INTRODUCTION

During the last decade, observations of stellar occultations by Uranus have led to the discovery (Elliot *et al.* 1977) and subsequent detailed kinematic characterization of the Uranian ring system (Elliot and Nicholson 1984). Among the significant results to come from stellar-occultation studies of this system are the discovery of eccentric and inclined rings, the first observations of narrow, sharp-edged rings, the first reliable determinations of Uranus' zonal gravity coefficients, J_2 and J_4, and refinements to Uranus' pole direction. The subkilometer precision of Earth-based occultation data, comparable to that obtainable from a spacecraft flyby, has both stimulated and provided a test of theoretical developments in the area of planetary ring dynamics (cf. Goldreich and Tremaine 1982). The combination of these Earth-based observations, acquired over the period 1977–1985, with stellar and radio occultation experiments carried out by the *Voyager* spacecraft in January 1986 has resulted in a kinematic model for the rings with an absolute accuracy of ~ 1 km and which fits the data with typical rms residuals of a few hundred meters (French *et al.* 1987). Despite the availability of the *Voyager* observations, there remains a need for continued Earth-based observations. Several questions concerning the origin of dynamical perturbations to the rings can only be answered by extending the time base of high-quality occultation data, and further refinements to the planet's gravity field depend on determining apsidal and nodal precession rates of individual rings with even higher precision than is currently available (~ 1 part in 10^4).

At present, Earth-based stellar-occultation observations provide the only source of information concerning the putative Neptunian rings, or arcs. Following the initial discovery of such material in 1984 (Hubbard *et al.* 1986), re-examination of previous stellar-occultation recordings (Guinan *et al.* 1982; Hubbard 1986), as well as subsequent occultation observations (Covault *et al.* 1986; Cooke *et al.* 1985; Sicardy *et al.* 1985), have provided additional evidence for the existence of incomplete rings or arcs around Neptune. Approximately 20% of the ~ 30 individual Neptune occultation observations reported to date have yielded secondary events which may be attributable to material in orbit around Neptune (Nicholson *et al.* 1988); three of these events were confirmed by independent observations at a second telescope. The upcoming encounter of *Voyager 2* with Neptune in August 1989 greatly increases the value of additional timely observations of the arcs. Such observations may permit a model of the system to be developed that could be used to guide and focus the spacecraft observations, and thus maximize their scientific value.

The great increase in the number of stellar occultations by both Uranus and Neptune observed in recent years has been a result of the availability of near-infrared photometers employing cooled InSb detectors, coupled with the realization that the reflected light from all of the Jovian planets is greatly reduced in the region λ 2.0–2.4 μm by strong H_2 and CH_4 absorption (cf. Fink and Larson 1979). The majority of stellar-occultation observations for these planets are carried out using standard *K* filters ($\lambda_0 = 2.2\,\mu$m, $\Delta\lambda = 0.4\,\mu$m), which are well matched to the planetary absorption bands. An additional factor in the number of observable occultations has been the proximity of both planets to the galactic plane, resulting in a greatly increased density of background stars. Unfortunately, no sufficiently deep λ 2.2 μm sky survey presently exists that would permit direct identification of suitable near-infrared occultation candidates. As a result, all previous searches for such candidates have employed either blue- or yellow-sensitive plates taken with astrographic telescopes (see, for example, Klemola *et al.* 1981; Mink *et al.*

[a)] Visiting Astronomer at the Infrared Telescope Facility, which is operated by the University of Hawaii under contract to the National Aeronautics and Space Administration.

 0004-6256/88/020562-14$00.90

1981; Mink and Klemola 1985). While these surveys have indeed revealed many occultation opportunities, it is also apparent that they have missed many highly reddened stars which fall below their magnitude cutoff (typically $m_V \simeq 14$), but which would provide excellent-quality data at λ 2.2 μm. The increased interstellar extinction at low galactic latitudes may be expected to exacerbate this situation at the present epoch for Uranus and Neptune, and suggests that a search at near-infrared wavelengths might turn up many more occultation candidates.

In an attempt to test this hypothesis, we commenced in 1984 a program of automated searches for stellar-occultation candidates, using a series of survey plates taken with the 1.2 m U.K. Schmidt Telescope at Siding Spring Observatory, Australia. As well as B and V plates similar to those of the Palomar Sky Survey, the southern sky survey includes IIIa-F and IV-N plates, with filters chosen to yield passbands approximating those of the near-infrared R and I bands in the Cousins photoelectric system (Cousins 1980; Reid and Gilmore 1982). The effective wavelengths of these plate–filter combinations are ~6500 and ~8000 Å, for R and I, respectively. An initial search for Neptune occultation candidates in the period 1984–1985 (the planet crossed the galactic plane in 1984) was carried out using a single set of plates in all four colors, with the stellar positions and magnitudes measured by the automatic COSMOS plate-scanning machine (Gilmore 1984). This trial survey confirmed both our expectation that many highly reddened stars missed in visual surveys would be identified, and that astrometry of sufficient accuracy ($\lesssim 0.3''$) was possible with these plates.

At least five of the Neptune occultations predicted in this trial survey have been successfully observed (Nicholson *et al.* 1988; Hubbard *et al.* 1987; Lellouch *et al.* 1986). Particularly noteworthy was a star occulted on 20 August 1985, observed at five different sites, which at $K = 6.4$ is among the brightest stars for which occultation data have been obtained. The Schmidt-plate-derived magnitudes were $I = 11.9$, $R = 14.9$, and $V = 18.2$, putting this star well below the limits for visual surveys and illustrating nicely the value of near-infrared searches.

In this paper, we present the first published results of this program, in the form of stellar-occultation predictions for Uranus and Neptune during the period 1987–1990. Our lists contain 167 Uranus occultation candidates, down to an estimated K magnitude of 12.0, and 80 Neptune candidates down to $K = 13.0$. This may be compared with a combined total of 60 candidates for Uranus and Neptune given by Mink and Klemola (1985) for the same period, down to a limiting magnitude, $m_V \simeq 14$. *JHK* photometry for most of our Neptune candidates indicates that the newly identified stars are, on average, at least as bright at λ 2.2 μm as those previously identified, with a significant number brighter than $K = 10.0$. Despite the increased number of occultation candidates identified in this survey, it is by no means complete. One measure of completeness is provided by the fraction of stars listed by Mink and Klemola (1985) recovered in our work: 45 out of 60, or 75%. The reasons for this incompleteness are discussed below.

The 1987 predictions are included here for reference, although it is recognized that most will have already occurred by the time of publication. Predictions for these particular events were circulated privately in advance of publication, and several researchers at the time of writing either have already observed, or plan to observe, some of these events.

II. PLATE MEASUREMENTS

Four pairs of R and I plates, taken with the U.K. Schmidt Telescope during the period 1982–1985, were used in the present survey of candidates for stellar occultations by Uranus and Neptune. The track of Uranus during 1987–1990 is covered by three fields, while Neptune's track for the same period is covered by two. One of the plate pairs covers both Uranus in 1989–1990 and Neptune in 1987–1988. Adjacent fields for a given planet overlap by ~5 min in R.A., so that no internal gaps in the coverage exist. However, portions of the 1987 Uranus and 1990 Neptune tracks lie outside the region covered by the available plates. The range in R.A. covered by our survey for each planet is as follows:

Uranus: $17^h31^m \leqslant \alpha_{1950} \leqslant 18^h43^m$;

Neptune: $18^h17^m \leqslant \alpha_{1950} \leqslant 18^h56^m$.

Neptune crossed the galactic plane at $\alpha \simeq 18^h01^m$ in 1984, while Uranus follows at $\alpha \simeq 17^h57^m$ in 1988. The densest visible star fields, however, lie to the south of the plane at $18^h10^m \lesssim \alpha \lesssim 18^h33^m$, in regions traversed by Neptune in 1986–1987 and Uranus in 1989–1990. The present survey, therefore, covers what may well be the richest areas for occultations by either planet in this century.

For each plate pair, a strip of width 40′ or 50′ in Dec. extending across the entire 6° field was scanned with the APM automatic plate-measuring machine at the University of Cambridge. Using a merged catalog compiled from the SAO, Perth 70, and Perth 80 star catalogs, a set of ~30 reference stars was first identified on each plate to establish a rough positional transformation from plate coordinates to R.A. and Dec. Because of differences between the algorithm used to locate the centers of the reference stars (which employs the diffraction spikes) and that used to locate the centers of the program stars (image centroid), combined with off-axis aberrations introduced by the telescope optical system, there exist systematic errors in the derived rough positions at the $1''$–$2''$ level. Differential thermal expansion between the plate holder and the measuring interferometer during the period of measurement may further contribute to systematic positional errors. We describe the procedure used to remove these systematic errors below. A total of 22 361 stars on two plate pairs were measured for Neptune, and 35 765 stars on three plate pairs for Uranus.

As well as determining the centroid and (uncalibrated) stellar magnitude of each image, the scanning algorithm estimates its departure from circularity. Noticeably noncircular images were rejected as indicating probable mergers of two or more individual stellar images. Because of the very crowded fields encountered in this survey, this restriction has the effect of rejecting most of the brightest stars on the plates, which show the largest images, as well as a certain fraction of all stars which is approximately independent of apparent magnitude over the range of interest here. This omission of the brightest stars is unlikely to be serious, inasmuch as such stars are very likely to appear in the lists of Mink and Klemola (1985). The fainter merged images would yield unreliable astrometry. Also rejected were objects identified on only one plate of the pair, thus eliminating plate defects of stellar appearance.

R and I magnitudes were estimated for each identified star, based on the measured photographic density and an assumed mean stellar-image profile. The magnitudes so determined are believed to conform fairly closely ($\pm$ 0.1–0.2

mag) to a true linear scale in magnitude, but with a rather uncertain and probably spatially variable zero point. The spatial variations arise from the fact that the fields of interest are crowded and contain several large H II regions. Thus substantial photographic background density variations occur on all spatial scales. The rapid-scanning mode of the measuring machine employed for these large area scans necessitated a simple algorithm for local background determination, which does not lead to high photometric precision in these circumstances. Merging of fainter stellar images with those of bright stars may also lead to some magnitude-dependent errors in the photometric calibration.

No suitable sequences of standard stars are available in these fields to provide a good absolute calibration of the machine magnitudes. We attempt below to establish an empirical calibration of the R and I magnitudes, based on published CCD photometry (French *et al.* 1986) for Uranus occultation candidates identified by Mink and Klemola (1985). The limiting magnitudes for the stars included in the present work are, approximately, $I = 15$ and $R = 16$, though two of the Uranus plates were scanned as deep as $I = 16$.

III. IDENTIFICATION OF OCCULTATION CANDIDATES

As a first step in selecting candidates for planetary occultations, we established within each region scanned a diagonal strip of width 10′ or 14′ in Dec., which encompasses the complete track followed by the planet across that plate. All stars falling outside this strip were rejected, and the remainder were sorted in order of increasing R.A. to facilitate the search procedure. Our five final catalogs compiled in this manner contain 6372 stars for Neptune and 8353 for Uranus. Because of the necessity to perform plate-dependent positional and photometric corrections to these data, the separate plate catalogs were not merged into a single catalog for each planet.

In order to correct for the systematic errors in the measured stellar positions alluded to above, we have employed the extensive set of star positions determined by Mink and Klemola (1985) from plates taken with the Carnegie double astrograph at Lick Observatory in 1982–1983. These unpublished lists contain a total of ~5000 stars, all lying within a few arcminutes of the tracks followed by Uranus and Neptune, and formed the basis of the published predictions in Mink and Klemola (1985). They were kindly provided to us for the current purpose in machine-readable form by D. Mink. Within each of our five diagonal strips, a computer search was carried out to match the stars in the Lick list with those in our sorted catalog. Typically, ~400 Lick stars were identified within each strip. Plots of the residuals in R.A. or Dec. vs. R.A. showed significant but smoothly varying systematic errors in the APM positions relative to the astrographic positions, with errors in Dec. amounting to as much as 2.5″.

For each strip, fourth-order polynomials were fitted to the measured residuals as functions of R.A., and subsequently used to correct the APM positions within the computer program used to search for occultation candidates. The rms residuals from these fitted polynomials provide an objective measure of the *internal* random errors in both the Lick measurements and in the APM measurements. The former are estimated by Mink and Klemola (1985) at 0.1″–0.2″ for well-exposed images. Averaged over all five strips surveyed, our mean rms residuals are 0.18″ in R.A. and 0.19″ in Dec., with the largest values being 0.22″ in R.A. and 0.23″ in Dec. We conclude that the *internal* random errors in the APM positions are comparable with those of the astrographic measurements, and quite adequate for the purpose of predicting stellar-occultation opportunities.

In selecting those stars that Uranus or Neptune would occult or approach closely, we employed planetary astrometric ephemerides calculated at daily intervals by M. Standish of the Jet Propulsion Laboratory. The specific ephemeris used is designated DE-118, and is dynamically equivalent to the ephemeris published in current editions of the *Astronomical Almanac*. (DE-118 differs only in being referred to the equator and equinox of 1950.0, rather than J2000, and thus matches our star positions, which are referred to star catalogs of equinox 1950.0.) The Uranus ephemeris includes corrections to the planet's position relative to the system barycenter due to the five large satellites. The Neptune ephemeris employed is barycentric; Triton's mass is unknown, but the estimated barycenter offset of Neptune is $\lesssim 0.02''$.

A computer program stepped along the planetary ephemeris, at intervals of 1 day, comparing each star position in turn with the linearly interpolated planetary track. All stars lying within a perpendicular distance of $\pm 5''$ from the track were identified, numbered, and selected for further study. Except for regions close to the planets' two stationary points in each year, this procedure made it unnecessary to check any given star more than once. The same program estimated the time of closest geocentric approach of the planet to the star, their minimum geocentric separation (designated "p" in the tables), and the velocity of the planet in the 'sky plane,' all based on a linear interpolation of the daily ephemeris. In a few cases it was necessary to make manual adjustments to the final results, either to remove duplications or to correct the date of events occurring near 0^h UT. Only within a week or two of the stationary points does this linear-interpolation scheme lead to significant errors in the predicted close-approach times or distances. Even at these locations, however, interpolation errors are less important than errors in either the stellar positions or in the planetary ephemeris, both of which are estimated at ~0.3″.

A final computer program checked the local circumstances for observations of each of the events selected above at a network of 11 stations distributed quasi-uniformly around the world, and applied empirical corrections to the measured machine magnitudes as discussed below. Our final merged lists of candidates for occultations by Uranus and Neptune are presented in Tables I and II, respectively. In order to avoid potential confusion with the numbering system of Mink and Klemola (1985), we have assigned our stars designations starting at u1001 and n1001.

In assembling these lists, the following criteria were adopted in an attempt to eliminate those events that were unlikely to yield useful data, without deleting any potentially observable occultations.

(i) A maximum geocentric miss distance of 4″ for Uranus and 1.5″ for Neptune. The limit for Uranus approximately matches the projected radius of the ϵ ring at opposition (3.9″), while the limit for Neptune is slightly greater than the planet's opposition radius of 1.2″. The Neptune limit corresponds to the maximum projected distance perpendicular to the planet's track of an equatorial ring at a distance of ~59 000 km, or $2.35R_N$. While arcs at greater distances have been reported, the most useful data require observations of a planetary occultation in order to accurately recon-

TABLE I. Stellar occultation predictions for Uranus. Close-approach time (ET) and minimum separation (p) are geocentric. The sky-plane velocity is given in km/s. I magnitudes and $R-I$ colors are derived from the plate measurements, as described in the text. Estimated K magnitudes are based on the empirical calibration of Fig. 3. Events designated U34, U35, etc., were also identified by Mink and Klemola (1985). Also included in the table, but left unnumbered, are those Mink and Klemola stars that were not recovered in the present survey.

Event #		Date	E.T.	p(")	V_sky	R.A.(1950)	DEC.(1950)	I	R-I	K_est	Observable at
u1001		1987 Jan 26	13:57	-1.2	29.76	17 35 58.305	-23 26 38.80	12.7	0.8	11.0	Pal.
u1002		1987 Jan 28	19:33	0.5	29.08	17 36 26.793	-23 26 55.10	13.9	1.9	10.4	
u1003		1987 Jan 31	2:49	-1.2	28.02	17 36 55.411	-23 27 14.49	14.1	2.2	10.4	SAAO
u1004		1987 Feb 5	13:13	0.1	26.12	17 37 59.708	-23 27 52.27	12.8	1.0	10.7	Pal. KPNO
u1005		1987 Feb 6	3:14	-3.4	25.73	17 38 6.338	-23 27 59.67	14.9	2.1	11.2	SAAO
u1006		1987 Feb 10	12:31	-0.6	24.10	17 38 54.326	-23 28 25.24	12.3	1.3	9.8	KPNO
u1007		1987 Feb 19	13:28	-3.5	20.18	17 40 22.393	-23 29 18.89	14.9	3.1	9.7	Pal.
u1008	U34	1987 Feb 26	15:18	-0.4	16.90	17 41 20.381	-23 29 48.76	12.7	0.8	11.0	M.K.
u1009		1987 Mar 5	0:43	-0.2	13.95	17 42 3.850	-23 30 13.54	14.7	1.7	11.6	SAAO
u1010	U35	1987 Mar 6	18: 5	-1.1	12.95	17 42 14.030	-23 30 20.44	12.4	0.7	10.8	AAO
u1011	U36	1987 Apr 1	3:55	-0.3	0.27	17 43 27.139	-23 31 14.43	11.1	0.8	9.3	Rio Ten. Pic. SAAO
u1012		1987 Apr 10	1: 5	-1.6	4.59	17 43 17.989	-23 31 20.93	15.0	2.3	11.1	SAAO
u1013		1987 Apr 10	7:53	-3.6	4.59	17 43 17.389	-23 31 22.93	14.4	2.6	9.9	CTIO Rio
u1014	U37	1987 Apr 16	2:42	-2.7	7.34	17 43 1.759	-23 31 21.53	9.6	1.0	7.6	Rio Ten. Pic. SAAO
u1015		1987 Apr 23	13:38	3.1	10.38	17 42 31.240	-23 31 10.34	14.6	3.5	8.9	M.K. AAO
u1016		1987 Apr 24	2:24	-1.9	10.80	17 42 28.640	-23 31 14.74	14.1	2.0	10.6	Rio Ten. Pic. SAAO
u1017	U38	1987 Apr 24	14:24	3.6	10.80	17 42 26.130	-23 31 8.64	13.0	0.2	12.1	M.K. AAO
u1018		1987 May 4	2:11	0.4	14.63	17 41 29.721	-23 30 56.36	14.1	2.8	9.5	CTIO Rio Ten. Pic. SAAO
u1019		1987 May 7	5:55	-2.1	15.65	17 41 7.442	-23 30 51.76	12.7	1.8	9.5	CTIO Rio
u1020		1987 May 12	23:52	-1.0	17.20	17 40 22.883	-23 30 35.29	14.3	2.4	10.2	Rio Ten. Pic. SAAO
u1021		1987 May 13	22: 7	2.4	17.49	17 40 15.243	-23 30 29.09	13.2	3.7	7.2	SAAO Kav.
u1022		1987 May 20	2:32	3.1	19.32	17 39 21.375	-23 30 7.62	13.1	1.5	10.3	CTIO Rio Ten. Pic. SAAO
u1023		1987 May 23	2:12	3.0	20.00	17 38 53.716	-23 29 56.34	12.7	1.1	10.6	CTIO Rio Ten. Pic. SAAO
u1024		1987 May 27	21:27	2.8	20.78	17 38 7.308	-23 29 36.46	14.4	1.9	11.0	SAAO Kav.
u1025	U39	1987 May 29	15:21	1.7	21.11	17 37 49.919	-23 29 29.67	12.6	0.5	11.3	PMO AAO
	U40	1987 May 31	14:11	2.0	21.40	17 37 30.213	-23 29 20.35				M.K. PMO AAO
u1026		1987 May 31	21:17	-1.1	21.41	17 37 27.200	-23 29 21.98	13.3	1.7	10.2	SAAO Kav.
u1027		1987 Jun 3	3:49	2.3	21.79	17 37 3.891	-23 29 7.59	14.1	1.9	10.7	CTIO Rio Ten. SAAO
	U41	1987 Jun 4	11:10	1.2	21.90	17 36 50.350	-23 29 2.17				M.K. Pal. KPNO AAO
u1028		1987 Jun 5	2:17	0.5	22.00	17 36 43.792	-23 28 59.69	14.3	1.3	11.8	CTIO Rio Ten. Pic. SAAO
u1029	U42	1987 Jun 21	18:26	0.2	22.42	17 33 46.435	-23 27 25.59	11.0	0.5	9.6	SAAO Kav. PMO AAO
u1030		1987 Jun 27	1:54	3.7	21.99	17 32 50.340	-23 26 49.08	9.6	0.3	8.6	CTIO Rio Ten. SAAO
u1031		1987 Jun 27	8:44	3.5	21.99	17 32 47.370	-23 26 47.47	13.8	1.1	11.6	M.K. Pal. KPNO CTIO AAO
u1032		1987 Jul 3	1:25	-0.9	21.22	17 31 48.796	-23 26 15.88	14.6	1.7	11.5	CTIO Rio Ten. SAAO
u1033		1987 Oct 23	19: 9	-2.6	24.65	17 30 51.752	-23 25 55.93	12.6	2.1	9.0	SAAO
u1034		1987 Oct 25	19:56	3.7	25.45	17 31 14.100	-23 26 5.44	12.0	1.7	8.8	Ten.
u1035		1987 Oct 28	21:28	2.5	26.61	17 31 49.006	-23 26 30.78	14.3	4.0	7.9	
u1036		1987 Nov 1	3: 0	1.4	28.06	17 32 27.402	-23 26 58.01	14.0	1.3	11.5	
u1037		1987 Nov 4	22:23	1.0	29.09	17 33 14.607	-23 27 29.63	14.1	2.0	10.5	Rio
u1038		1987 Nov 10	7:59	1.6	31.00	17 34 24.951	-23 28 14.14	14.1	1.9	10.7	
u1039		1987 Nov 12	14:34	3.6	31.58	17 34 55.679	-23 28 31.27	14.0	2.1	10.3	
u1040		1987 Nov 17	8:12	0.6	32.94	17 36 1.545	-23 29 14.10	13.3	2.8	8.7	
u1041		1987 Nov 18	11:42	1.6	33.19	17 36 17.854	-23 29 22.70	13.9	2.5	9.6	
u1042		1987 Nov 23	9:19	2.1	34.33	17 37 29.020	-23 30 2.98	12.1	1.7	9.0	
u1043		1987 Nov 28	9:50	-1.0	35.26	17 38 44.026	-23 30 46.94	14.2	3.1	9.0	
u1044		1988 Jan 10	10:24	-3.0	35.01	17 49 55.021	-23 35 22.93	12.3	3.0	7.4	
u1045		1988 Jan 21	5: 3	3.1	32.56	17 52 32.344	-23 35 57.88	14.9	4.4	7.7	
u1046		1988 Jan 31	5: 9	-1.9	29.55	17 54 47.287	-23 36 31.64	10.8	0.3	9.7	
u1047		1988 Jan 31	7:44	3.3	29.55	17 54 48.677	-23 36 26.79	12.8	0.4	11.6	Rio
u1048		1988 Feb 23	18:45	3.4	20.39	17 59 6.698	-23 37 8.08	14.2	1.2	12.0	AAO
u1049	U43	1988 Mar 8	16:14	3.6	13.73	18 0 51.273	-23 37 22.92	12.4	0.4	11.2	AAO
u1050		1988 Apr 19	12: 9	3.8	7.09	18 1 49.311	-23 38 8.68	13.3	0.9	11.5	M.K. Pal.
	U44	1988 Apr 26	7:48	3.5	10.10	18 1 22.202	-23 38 17.62				KPNO CTIO Rio
u1051	U45	1988 Apr 27	15:59	0.0	10.54	18 1 15.752	-23 38 22.80	12.5	0.3	11.4	AAO
u1052		1988 May 12	13:48	-4.0	16.08	17 59 41.956	-23 38 43.36	13.4	1.1	11.2	M.K. AAO
u1053	U46	1988 May 12	17:08	-1.8	16.08	17 59 40.906	-23 38 41.63	13.1	0.1	12.4	Kav. PMO AAO
u1054		1988 May 13	23:55	-1.7	16.40	17 59 31.067	-23 38 42.37	14.3	1.9	10.9	SAAO
u1055		1988 May 24	23: 2	3.2	19.41	17 57 57.482	-23 38 44.91	12.4	0.5	11.1	SAAO Kav.
u1056		1988 Jun 11	6:35	3.0	22.22	17 55 4.781	-23 38 44.24	13.5	2.0	10.0	Pal. KPNO CTIO Rio
u1057		1988 Jun 28	5:53	1.9	22.22	17 52 4.035	-23 38 27.55	13.1	0.5	11.8	M.K. Pal. KPNO CTIO Rio

TABLE I. (continued)

Event #		Date	E.T.	p(")	V_sky	R.A.(1950)	DEC.(1950)	I	R-I	K_est	Observable at
u1058		1988 Jun 29	13:12	3.1	22.14	17 51 50.306	-23 38 24.41	13.3	0.6	11.7	M.K. PMO AAO
u1059		1988 Jul 21	6:22	2.2	18.27	17 48 19.050	-23 37 42.42	12.2	1.4	9.5	M.K. Pal. KPNO CTIO
u1060		1988 Jul 30	19:34	-3.9	15.59	17 47 2.979	-23 37 27.54	13.3	0.7	11.6	SAAO Kav.
u1061		1988 Sep 27	11:13	3.1	11.04	17 45 38.169	-23 36 48.88	13.9	1.4	11.2	PMO AAO
u1062		1988 Oct 16	16: 6	-0.2	20.12	17 47 51.459	-23 37 32.39	13.4	0.6	12.0	
u1063		1988 Oct 19	16:24	-2.6	21.44	17 48 19.050	-23 37 42.42	12.2	1.4	9.5	
u1064		1988 Nov 9	20:22	-3.8	29.58	17 52 16.623	-23 38 38.87	12.1	0.9	10.1	
u1065		1988 Nov 14	6:34	3.0	31.14	17 53 14.744	-23 38 42.55	12.4	3.2	7.0	
u1066		1988 Nov 15	8:15	1.8	31.43	17 53 29.164	-23 38 46.21	11.9	1.3	9.4	
u1067		1988 Nov 16	9:44	3.1	31.72	17 53 43.608	-23 38 47.28	13.4	0.7	11.8	AAO
u1068		1988 Dec 3	18:30	0.5	35.49	17 57 55.612	-23 39 18.91	11.0	0.6	9.5	
u1069		1989 Jan 22	6:36	3.6	33.15	18 10 38.936	-23 38 26.25	12.8	1.9	9.5	
u1070		1989 Jan 26	6:28	3.9	32.11	18 11 35.108	-23 38 14.58	13.9	1.2	11.6	
u1071		1989 Feb 2	9:21	-0.5	30.03	18 13 10.750	-23 37 57.33	13.6	0.8	11.8	CTIO
u1072		1989 Feb 4	0:44	1.6	29.37	18 13 31.890	-23 37 50.13	13.4	0.8	11.7	
u1073		1989 Feb 7	21: 3	1.1	28.33	18 14 19.940	-23 37 38.44	13.9	1.2	11.6	
u1074		1989 Feb 8	9:34	-3.3	27.97	18 14 26.290	-23 37 41.24	12.9	0.9	11.0	
u1075		1989 Feb 9	10:33	-3.5	27.60	18 14 38.840	-23 37 38.14	10.6	1.5	7.7	
u1076		1989 Feb 9	17:57	2.6	27.60	18 14 42.520	-23 37 31.04	14.1	1.2	11.7	AAO
u1077		1989 Feb 12	2:32	0.0	26.47	18 15 10.229	-23 37 26.24	11.9	0.8	10.1	SAAO
u1078		1989 Feb 19	7:31	0.9	23.65	18 16 29.276	-23 37 3.29	8.7	0.9	6.9	CTIO Rio
u1079		1989 Feb 19	21:27	0.8	23.65	18 16 35.266	-23 37 1.69	14.4	2.1	10.8	PMO
u1080		1989 Mar 1	20:34	-4.0	19.25	18 18 8.338	-23 36 39.54	13.8	1.6	10.9	PMO
u1081	U47	1989 Mar 6	7:35	0.5	16.89	18 18 43.752	-23 36 24.83	11.5	0.6	10.0	CTIO Rio
u1082	U48	1989 Mar 12	15:22	-3.1	13.95	18 19 26.971	-23 36 16.63	13.6	0.9	11.7	M.K. AAO
u1083	U49	1989 Mar 13	10:50	-0.4	13.46	18 19 31.890	-23 36 12.64	11.2	1.0	9.2	
u1084	U50	1989 Mar 14	19:53	-0.2	12.96	18 19 39.940	-23 36 10.35	11.7	0.9	9.8	PMO
u1085		1989 Mar 19	5: 0	-1.2	10.46	18 20 2.768	-23 36 6.19	12.8	0.3	11.8	Rio Ten. Pic.
u1086		1989 Apr 4	12:50	-1.3	2.37	18 20 50.245	-23 36 4.45	13.4	0.8	11.7	M.K.
u1087		1989 May 8	13:12	-2.1	13.08	18 19 20.301	-23 37 31.52	12.4	2.1	8.7	M.K. AAO
u1088		1989 May 17	9: 7	1.5	16.20	18 18 19.913	-23 38 5.06	13.4	0.8	11.7	M.K. Pal. KPNO CTIO
u1089		1989 May 17	13:47	-1.6	16.20	18 18 18.447	-23 38 9.02	12.5	0.9	10.6	M.K. AAO
u1090		1989 May 20	17: 5	2.4	17.12	18 17 53.919	-23 38 18.97	13.6	1.6	10.7	Kav. PMO AAO
u1091	U51	1989 May 21	11:56	1.4	17.41	18 17 47.563	-23 38 23.45	12.2	0.3	11.1	M.K. AAO
u1092		1989 May 27	9:55	3.0	19.02	18 16 56.991	-23 38 48.73	13.7	1.3	11.3	M.K. Pal. KPNO CTIO
u1093		1989 May 28	0: 9	-0.7	19.02	18 16 51.701	-23 38 55.21	12.4	2.0	8.8	Rio Ten. Pic. SAAO
u1094		1989 May 29	20:34	-3.4	19.50	18 16 34.856	-23 39 6.29	12.6	0.8	10.9	SAAO Kav.
u1095	U52	1989 Jun 2	11:59	-0.9	20.36	18 16 0.597	-23 39 20.42	11.1	0.7	9.4	M.K. AAO
	U53	1989 Jun 10	15:46	2.9	21.70	18 14 39.570	-23 39 53.12				Kav. PMO AAO
u1096		1989 Jun 11	12:26	-3.1	21.77	18 14 30.750	-23 40 2.84	13.5	0.8	11.7	M.K. AAO
u1097		1989 Jun 13	1: 8	1.5	21.99	18 14 14.960	-23 40 4.84	12.9	1.1	10.6	CTIO Rio Ten. Pic. SAAO
u1098		1989 Jun 19	12:11	3.9	22.43	18 13 7.130	-23 40 29.02	13.0	0.8	11.2	M.K. AAO
u1099		1989 Jun 22	5:37	-2.7	22.53	18 12 38.159	-23 40 46.21	13.2	0.6	11.8	Pal. KPNO CTIO Rio
u1100	U54	1989 Jun 24	9:28	1.9	22.56	18 12 15.119	-23 40 49.70	13.2	0.1	12.5	M.K. Pal. KPNO CTIO AAO
u1101	U55	1989 Jun 28	15: 9	3.2	22.52	18 11 29.928	-23 41 3.38	12.1	0.6	10.6	Kav. PMO AAO
u1102		1989 Jun 30	20:49	2.3	22.44	18 11 6.167	-23 41 11.76	13.7	0.9	11.8	SAAO Kav.
u1103		1989 Jul 1	21:40	2.3	22.38	18 10 55.207	-23 41 15.16	12.9	1.0	10.9	Rio Ten. Pic. SAAO Kav.
u1104		1989 Jul 4	3: 7	3.6	22.17	18 10 31.746	-23 41 20.74	14.1	1.0	12.0	CTIO Rio Ten. SAAO
u1105		1989 Jul 14	23: 4	-1.1	20.85	18 8 41.433	-23 41 54.39	14.1	1.6	11.2	CTIO Rio Ten. Pic. SAAO
u1106		1989 Jul 18	24:15	3.4	20.10	18 8 2.511	-23 41 58.48	13.6	0.9	11.8	CTIO Rio Ten. Pic. SAAO
u1107		1989 Aug 15	19:23	-1.9	11.50	18 4 32.618	-23 42 35.39	13.5	0.9	11.5	SAAO Kav.
u1108		1989 Sep 3	17:10	-1.0	3.15	18 3 28.579	-23 42 36.41	13.1	0.9	11.2	SAAO Kav.
u1109		1989 Oct 10	16:15	-2.2	15.16	18 5 8.608	-23 42 15.68	11.2	0.8	9.5	
u1110		1989 Oct 28	22:10	3.9	23.33	18 7 44.401	-23 41 41.27	11.4	0.4	10.3	Rio
u1111		1989 Nov 5	9:21	-1.1	26.54	18 9 5.663	-23 41 28.90	13.6	0.7	11.9	AAO
u1112		1989 Nov 9	8:43	-2.9	28.00	18 9 52.535	-23 41 19.62	11.8	1.2	9.5	
u1113		1989 Nov 11	13:36	-0.5	28.70	18 10 19.526	-23 41 10.64	12.2	0.8	10.4	Kav.
u1114		1989 Nov 12	0:50	3.4	29.04	18 10 25.326	-23 41 5.24	13.3	0.6	11.9	CTIO
u1115		1989 Nov 12	13: 2	-2.4	29.04	18 10 31.706	-23 41 9.44	11.3	1.8	8.1	Kav.
u1116		1989 Nov 18	5: 0	-0.3	30.96	18 11 44.888	-23 40 47.78	11.1	0.5	9.8	
u1117		1989 Nov 20	15:13	3.2	31.55	18 12 17.469	-23 40 35.00	11.3	0.8	9.6	
u1118		1989 Nov 29	18:11	3.9	33.87	18 14 25.820	-23 39 54.34	12.2	1.9	8.8	
u1119		1990 Feb 1	21:34	-2.8	31.65	18 30 36.802	-23 31 55.64	13.6	1.0	11.6	
u1120		1990 Feb 11	9:51	-0.6	28.46	18 32 39.616	-23 30 30.78	13.6	1.1	11.4	
u1121		1990 Feb 17	0:11	-0.2	26.64	18 33 45.998	-23 29 44.13	10.9	1.2	8.5	Kav.
u1122		1990 Feb 19	10:59	-1.6	25.47	18 34 13.498	-23 29 26.15	13.2	1.2	10.9	
u1123		1990 Feb 24	21:14	-1.2	23.42	18 35 10.897	-23 28 44.81	13.0	1.3	10.5	PMO
u1124		1990 Feb 27	5:55	2.2	22.13	18 35 34.236	-23 28 24.73	12.7	1.1	10.5	Rio Ten.
u1125	U56	1990 Mar 18	3: 3	2.5	13.22	18 38 2.318	-23 26 39.91	13.8	1.2	11.5	SAAO
u1126	U57	1990 Apr 3	18: 5	1.1	5.14	18 39 10.468	-23 26 2.59	11.3	0.7	9.6	AAO

TABLE I. (continued)

Event #		Date	E.T.	p(")	V_sky	R.A.(1950)	DEC.(1950)	I	R-I	K_est	Observable at
u1127		1990 Apr 29	13: 1	-1.7	7.47	18 38 54.534	-23 26 57.57	13.5	1.3	10.9	M.K. AAO
u1128	U58	1990 May 11	3:47	-1.6	12.45	18 38 1.478	-23 28 1.81	12.8	1.3	10.3	CTIO Rio Ten. SAAO
u1129		1990 May 15	13:42	3.8	13.94	18 37 34.643	-23 28 26.27	13.2	1.0	11.1	M.K. AAO
u1130		1990 May 20	19:32	2.8	15.69	18 36 58.499	-23 29 5.73	13.2	1.2	10.9	Kav. PMO AAO
u1131	U59	1990 May 24	5:32	-0.6	16.96	18 36 32.592	-23 29 35.90	13.1	1.1	11.0	CTIO Rio
u1132	U60	1990 May 24	19:51	0.0	16.96	18 36 27.882	-23 29 40.09	13.4	1.3	11.0	SAAO Kav. PMO AAO
u1133	U61	1990 May 27	9:14	3.0	17.83	18 36 7.114	-23 29 57.87	11.0	0.9	9.0	M.K. Pal. KPNO CTIO
u1134		1990 Jun 4	14:46	3.8	19.81	18 34 54.668	-23 31 7.09	13.2	0.9	11.3	M.K. PMO AAO
u1135	U62	1990 Jun 9	8:43	-3.4	20.79	18 34 9.568	-23 31 55.85	13.9	0.6	12.4	M.K. Pal. KPNO CTIO Rio
	U63	1990 Jun 12	23: 9	3.3	21.30	18 33 33.989	-23 32 20.96				Rio Ten. Pic. SAAO Kav.
	U64	1990 Jun 17	22:53	2.4	22.00	18 32 43.223	-23 33 5.94				Rio Ten. Pic. SAAO Kav.
u1136	U65	1990 Jun 21	10:49	-2.7	22.31	18 32 6.855	-23 33 41.66	10.5	1.5	7.8	M.K. Pal. KPNO CTIO AAO
	U66	1990 Jun 21	17:46	-2.1	22.30	18 32 3.815	-23 33 43.55				SAAO Kav. PMO AAO
u1137		1990 Jun 25	6:21	-2.5	22.52	18 31 26.664	-23 34 14.35	13.1	1.5	10.4	Pal. KPNO CTIO Rio
u1138		1990 Jun 29	8:38	-2.2	22.59	18 30 43.212	-23 34 48.64	12.8	1.0	10.7	M.K. Pal. KPNO CTIO AAO
u1139	U67	1990 Jul 4	1:45	3.5	22.47	18 29 53.191	-23 35 21.44	13.5	1.0	11.5	CTIO Rio Ten. Pic. SAAO
u1140		1990 Jul 5	4: 6	2.2	22.42	18 29 41.600	-23 35 31.44	13.3	1.3	10.9	Pal. KPNO CTIO Rio Ten.
u1141		1990 Jul 9	4:35	1.8	22.14	18 28 59.429	-23 36 2.85	13.7	1.1	11.5	Pal. KPNO CTIO Rio
u1142	U68	1990 Jul 12	0:57	3.4	21.84	18 28 29.929	-23 36 22.36	12.4	0.7	10.7	CTIO Rio Ten. Pic. SAAO
u1143		1990 Jul 16	10:12	-3.8	21.32	18 27 45.419	-23 37 0.57	13.6	1.2	11.2	M.K. AAO
u1144		1990 Jul 26	18: 3	3.0	19.41	18 26 6.531	-23 37 58.53	13.4	1.3	11.0	SAAO Kav.
u1145	U69	1990 Jul 28	2:35	-0.4	18.93	18 25 54.372	-23 38 9.53	13.3	0.7	11.7	CTIO Rio Ten.
u1146	U70	1990 Jul 29	14:51	-0.2	18.67	18 25 41.072	-23 38 17.54	11.6	1.6	8.7	Kav. PMO AAO
u1147	U71	1990 Jul 31	11:58	-3.0	18.15	18 25 24.923	-23 38 30.15	13.6	0.7	11.9	M.K. PMO AAO
u1148	U72	1990 Aug 2	9:15	-1.7	17.59	18 25 9.164	-23 38 38.16	13.0	1.0	11.0	M.K. AAO
u1149	U73	1990 Aug 7	0:35	2.7	16.40	18 24 32.516	-23 38 54.97	11.1	0.7	9.6	CTIO Rio Ten. SAAO
u1150		1990 Aug 23	13: 4	-1.1	10.18	18 22 50.454	-23 39 52.40	13.1	1.5	10.3	PMO AAO
u1151	U74	1990 Aug 30	17:28	-3.5	7.15	18 22 22.007	-23 40 7.40	12.1	1.1	9.9	SAAO Kav.
	U75	1990 Sep 4	0:12	-1.1	5.10	18 22 10.076	-23 40 9.47				CTIO Rio Ten.
u1152		1990 Sep 19	20:20	3.8	2.38	18 22 0.429	-23 40 2.10	13.2	0.8	11.5	Ten. Pic. SAAO
u1153		1990 Sep 26	6:32	4.0	5.91	18 22 12.468	-23 39 52.20	12.6	1.1	10.4	M.K.
u1154		1990 Oct 2	0: 1	-1.4	8.42	18 22 30.966	-23 39 44.80	12.9	1.6	10.0	CTIO Rio
u1155		1990 Oct 2	4:21	-2.2	8.92	18 22 31.686	-23 39 45.10	13.3	1.4	10.7	Pal. KPNO
u1156	U76	1990 Oct 17	19:55	-1.0	16.31	18 23 59.099	-23 38 47.99	12.4	0.6	11.0	Ten. SAAO
u1157		1990 Oct 24	3:34	-1.2	19.59	18 24 48.815	-23 38 16.57	11.2	2.1	7.5	
u1158		1990 Oct 31	10:53	-1.8	22.68	18 25 55.862	-23 37 33.83	12.8	1.8	9.6	PMO AAO
u1159		1990 Nov 1	21:50	2.0	23.10	18 26 10.351	-23 37 20.52	12.3	1.2	9.9	Rio
u1160		1990 Nov 13	6:23	0.3	27.82	18 28 15.759	-23 35 57.86	12.6	1.6	9.7	
u1161		1990 Nov 23	23:54	-2.8	31.12	18 30 31.872	-23 34 24.04	12.5	1.0	10.5	
u1162		1990 Nov 26	7:31	2.5	31.98	18 31 3.173	-23 33 55.54	12.8	0.5	11.5	
u1163		1990 Nov 28	5:39	-1.4	32.51	18 31 29.614	-23 33 39.65	10.7	0.1	9.9	
u1164		1990 Nov 29	12: 8	-3.1	32.77	18 31 47.295	-23 33 28.06	12.8	1.4	10.2	
u1165		1990 Dec 6	10:45	3.0	34.37	18 33 26.598	-23 32 5.11	12.5	1.9	9.0	
u1166		1990 Dec 7	3:53	-1.2	34.58	18 33 37.068	-23 32 1.02	11.0	0.7	9.4	
u1167		1990 Dec 9	18:45	-3.1	34.96	18 34 15.768	-23 31 31.95	12.7	1.7	9.7	

Observatory codes:

M.K. = Mauna Kea, Pal. = Palomar, KPNO = Kitt Peak, CTIO = Cerro Tololo, Rio = Rio de Janiero, Ten. = Teneriffe, Pic. = Pic du Midi, SAAO = Sutherland, Kav. = Kavalur, PMO = Purple Mtn. Obs., AAO = Anglo-Australian Obs..

TABLE II. Stellar-occultation predictions for Neptune. Close-approach time (ET) and minimum separation (p) are geocentric. The sky-plane velocity is given in km/s. I magnitudes and $R-I$ colors are derived from the plate measurements, as described in the text. Estimated K magnitudes are based on the empirical calibration of Fig. 3. Events designated N41, N42, etc., were also identified by Mink and Klemola (1985). Also included in the table, but left unnumbered, are those Mink and Klemola stars that were not recovered in the present survey.

Event #		Date	E.T.	p(")	V_sky	R.A.(1950)	DEC.(1950)	I	R-I	K_est	Observable at
n1001		1987 Jan 16	15: 1	1.5	33.95	18 24 53.464	-22 18 21.74	13.8	0.5	12.5	
n1002		1987 Jan 27	0:53	0.0	31.89	18 26 27.859	-22 17 21.61	12.9	0.4	11.7	
n1003	N41	1987 May 23	9:24	0.9	18.31	18 30 15.342	-22 12 21.78	13.6	1.0	11.6	M.K. Pal. KPNO CTIO
n1004	N42	1987 May 27	17:37	0.8	19.42	18 29 51.422	-22 12 36.28	13.1	0.8	11.2	Kav. PMO AAO
	N43	1987 Jun 2	1:10	-0.6	20.80	18 29 20.108	-22 12 57.18				CTIO Rio Ten. Pic. SAAO
n1005		1987 Jun 16	21: 1	-0.1	23.16	18 27 43.856	-22 14 0.30	9.7	1.0	7.7	SAAO Kav.
n1006		1987 Jun 22	3:18	-1.2	23.72	18 27 7.607	-22 14 26.30	12.9	1.6	10.0	CTIO Rio Ten. SAAO
n1007		1987 Jun 24	6: 6	0.3	23.79	18 26 52.858	-22 14 35.11	13.5	0.6	12.0	Pal. KPNO CTIO Rio
n1008		1987 Jul 9	8:58	0.2	23.40	18 25 7.474	-22 15 51.33	13.4	1.4	10.7	M.K. Pal. KPNO CTIO AAO
n1009	N44	1987 Jul 10	16:24	0.7	23.30	18 24 58.514	-22 15 57.53	13.0	1.0	10.9	Kav. PMO AAO
n1010		1987 Jul 14	22:10	-1.0	22.83	18 24 29.906	-22 16 20.84	13.3	0.5	12.0	Rio Ten. Pic. SAAO Kav.
n1011		1987 Jul 28	19:26	-1.2	20.16	18 23 2.343	-22 17 30.37	12.1	1.8	8.8	SAAO Kav.
	N45	1987 Aug 15	1:40	0.2	14.70	18 21 34.080	-22 18 48.79				CTIO Rio Ten.
n1012		1987 Aug 29	7:49	-1.2	8.86	18 20 44.946	-22 19 47.43	13.2	0.8	11.4	M.K.
n1013		1987 Nov 2	18:51	0.4	22.48	18 22 51.984	-22 21 20.98	13.3	1.4	10.7	SAAO
n1014		1987 Nov 17	2: 5	0.1	28.21	18 24 32.926	-22 20 52.34	13.5	1.4	10.9	
n1015		1987 Nov 29	18: 0	-0.3	31.74	18 26 18.059	-22 20 9.31	12.5	0.7	10.9	
n1016		1987 Dec 2	18:56	0.5	32.42	18 26 45.028	-22 19 55.71	13.7	0.8	12.0	
n1017		1987 Dec 12	9: 1	1.1	34.36	18 28 13.455	-22 19 8.49	13.3	1.2	11.0	
n1018		1987 Dec 22	1:49	0.5	35.39	18 29 46.722	-22 18 13.19	11.4	2.7	6.8	
n1019		1987 Dec 26	9:28	-0.1	35.61	18 30 28.901	-22 17 46.28	13.1	1.2	10.7	
n1020		1988 Jan 1	7:38	0.3	35.69	18 31 26.921	-22 17 5.79	12.1	1.5	9.3	
n1021		1988 Jan 14	14:19	-1.4	34.62	18 33 35.552	-22 15 30.15	14.1	0.8	12.4	
n1022		1988 Jan 18	6: 3	0.8	34.10	18 34 10.070	-22 14 59.66	14.3	1.3	11.8	
n1023		1988 Feb 14	2: 9	0.4	26.78	18 37 58.729	-22 11 28.98	14.2	0.9	12.2	SAAO
n1024		1988 Feb 23	21:32	-1.2	23.20	18 39 6.687	-22 10 18.42	13.6	1.3	11.1	PMO
n1025		1988 Mar 1	23:35	-1.0	20.18	18 39 49.034	-22 9 30.08	12.4	1.7	9.3	Kav.
n1026	N46	1988 Mar 5	3: 5	0.3	18.39	18 40 5.870	-22 9 8.94	13.1	0.9	11.2	SAAO
n1027	N47	1988 May 11	5:13	0.4	13.74	18 40 42.487	-22 7 4.22	12.2	0.5	11.0	CTIO Rio Ten.
n1028		1988 May 26	9:42	-0.6	18.75	18 39 30.726	-22 8 1.94	13.7	0.9	11.8	M.K. Pal. KPNO CTIO
n1029		1988 Jun 14	14:21	0.9	22.84	18 37 33.041	-22 9 43.67	14.3	1.2	11.9	M.K. PMO AAO
n1030		1988 Jul 6	1:18	-0.3	23.80	18 35 4.678	-22 12 2.78	14.2	1.1	12.0	CTIO Rio Ten. Pic. SAAO
n1031	N48	1988 Jul 9	9:55	0.3	23.53	18 34 41.400	-22 12 24.45	12.6	1.3	10.0	M.K. Pal. KPNO AAO
n1032		1988 Jul 11	15:23	1.4	23.40	18 34 26.079	-22 12 38.16	14.3	1.4	11.7	Kav. PMO AAO
n1033		1988 Jul 19	16:55	1.5	22.33	18 33 32.122	-22 13 31.15	13.7	1.2	11.4	SAAO Kav. PMO AAO
n1034		1988 Jul 25	0:11	1.1	21.43	18 32 58.323	-22 14 5.75	13.5	1.1	11.4	CTIO Rio Ten. Pic. SAAO
n1035		1988 Jul 30	22:41	0.7	20.02	18 32 22.604	-22 14 43.15	14.6	1.5	11.8	Rio Ten. Pic. SAAO
	N49	1988 Aug 2	5:48	-0.1	19.30	18 32 9.461	-22 14 57.89				M.K. Pal. KPNO CTIO Rio
n1036		1988 Aug 6	13: 1	-1.5	18.14	18 31 46.043	-22 15 24.78	12.9	0.7	11.3	PMO AAO
n1037		1988 Aug 13	11:55	-0.5	15.85	18 31 11.694	-22 16 2.84	11.9	1.6	8.9	PMO AAO
	N50	1988 Aug 22	21:30	0.8	12.30	18 30 33.287	-22 16 49.59				Ten. Pic. SAAO
n1038		1988 Aug 25	9:45	0.1	11.24	18 30 24.786	-22 17 1.95	13.9	2.0	10.3	M.K. AAO
n1039		1988 Sep 2	16:15	1.5	7.78	18 30 2.162	-22 17 35.88	13.3	0.7	11.7	Kav.
n1040	N51	1988 Sep 12	20: 3	-0.3	3.17	18 29 46.722	-22 18 13.19	11.4	2.7	6.8	Ten. Pic. SAAO
n1041		1988 Oct 17	22:46	-0.5	14.50	18 30 45.406	-22 18 57.02	13.9	1.8	10.6	Rio
n1042	N52	1988 Oct 22	9:23	-0.3	16.85	18 31 5.089	-22 18 52.44	12.2	0.9	10.4	AAO
n1043		1988 Nov 5	6:48	1.2	23.08	18 32 22.652	-22 18 22.18	11.8	0.9	9.9	
n1044		1988 Nov 14	18: 3	0.1	26.60	18 33 28.250	-22 17 49.91	12.5	1.9	9.1	
n1045		1988 Nov 17	17:18	-1.1	27.75	18 33 50.690	-22 17 38.39	12.7	1.9	9.3	
n1046		1988 Nov 21	19:18	0.5	29.02	18 34 22.860	-22 17 17.46	13.8	1.4	11.2	Ten.
n1047		1988 Dec 3	3:25	-0.5	32.37	18 35 59.199	-22 16 14.50	10.3	0.7	8.7	
n1048		1988 Dec 3	14:29	-1.2	32.37	18 36 3.307	-22 16 12.20	11.8	1.2	9.4	
n1049		1988 Dec 6	0: 5	0.9	32.80	18 36 24.886	-22 15 54.52	12.9	1.4	10.3	
n1050		1988 Dec 7	14:57	-0.6	33.21	18 36 39.673	-22 15 45.03	14.3	0.9	12.4	
n1051		1988 Dec 14	1:45	-0.6	34.43	18 37 39.770	-22 14 58.77	14.3	1.4	11.6	
n1052		1988 Dec 14	22:33	-0.4	34.43	18 37 47.967	-22 14 52.11	13.5	0.2	12.5	
n1053		1988 Dec 22	19:54	-1.5	35.34	18 39 3.787	-22 13 50.32	13.7	1.2	11.4	
n1054	•	1988 Dec 23	18:16	0.3	35.46	18 39 12.843	-22 13 40.79	11.6	1.2	9.3	
n1055		1988 Dec 25	4:28	1.0	35.50	18 39 26.712	-22 13 28.07	12.8	0.9	10.9	
n1056		1988 Dec 30	7:39	1.1	35.74	18 40 16.845	-22 12 43.26	14.0	1.4	11.4	

TABLE II. (continued)

Event #		Date	E.T.	p(")	V_sky	R.A.(1950)	DEC.(1950)	I	R-I	K_est	Observable at
n1057		1988 Dec 30	15:51	-0.6	35.74	18 40 20.202	-22 12 41.87	13.3	1.1	11.0	
n1058		1989 Jan 2	13:39	-0.2	35.70	18 40 48.665	-22 12 15.28	13.9	1.5	11.1	
n1059		1989 Jan 24	12: 1	1.1	33.17	18 44 17.846	-22 8 43.24	14.1	1.4	11.5	
n1060		1989 Feb 19	1:43	0.9	25.38	18 47 47.293	-22 4 38.59	14.1	1.1	11.8	
n1061	N53	1989 Feb 21	18:26	1.2	24.53	18 48 5.933	-22 4 14.60	12.7	1.1	10.4	AAO
n1062		1989 Mar 8	23:45	0.6	18.09	18 49 35.727	-22 2 14.47	14.4	1.0	12.3	Kav.
n1063		1989 Mar 27	2:53	0.8	8.79	18 50 43.858	-22 0 29.85	12.7	2.9	7.9	SAAO
n1064		1989 Jun 11	7:54	-0.1	21.94	18 47 33.552	-22 3 3.09	14.0	1.0	12.0	M.K. Pal. KPNO CTIO Rio
	N54	1989 Jun 14	10:15	0.3	22.40	18 47 13.512	-22 3 25.22				M.K. Pal. KPNO CTIO AAO
n1065		1989 Jun 23	20:16	1.0	23.48	18 46 10.149	-22 4 36.86	14.4	1.2	12.1	SAAO Kav. AAO
n1066		1989 Jun 26	12:58	-1.2	23.71	18 45 51.538	-22 5 0.46	14.1	1.4	11.4	M.K. AAO
	N55	1989 Jul 8	0: 8	0.1	23.80	18 44 31.526	-22 6 32.61				CTIO Rio Ten. Pic. SAAO
n1067		1989 Aug 23	12:58	-0.5	13.06	18 40 3.486	-22 12 13.86	14.6	1.4	12.0	PMO AAO
n1068		1989 Aug 26	10:23	0.5	11.90	18 39 53.086	-22 12 28.85	14.3	0.9	12.4	M.K. AAO
n1069		1989 Sep 17	7:27	0.5	1.89	18 39 8.887	-22 14 0.33	14.1	1.0	12.0	M.K.
n1070	N56	1989 Oct 8	20:18	-0.9	8.79	18 39 30.296	-22 14 32.84	13.3	1.4	10.7	Ten. SAAO
n1071		1989 Nov 1	11:45	0.4	20.35	18 41 8.304	-22 13 49.69	14.4	1.3	11.9	AAO
n1072		1989 Dec 19	6:38	0.9	34.87	18 47 28.982	-22 8 19.29	13.9	1.3	11.4	
n1073		1989 Dec 23	14: 2	-1.4	35.30	18 48 10.383	-22 7 37.90	12.9	0.8	11.2	
n1074		1990 Jan 6	15:27	1.4	35.59	18 50 27.378	-22 5 1.92	11.5	1.1	9.4	
n1075		1990 Jan 9	14:49	0.3	35.48	18 50 56.319	-22 4 28.97	12.8	1.2	10.4	
	N57	1990 May 25	11: 0	-1.3	16.90	18 58 45.705	-21 52 29.92				M.K. Pal. KPNO
n1076		1990 Jun 25	13:28	-0.5	23.33	18 55 37.429	-21 56 42.31	14.4	1.0	12.3	M.K. PMO AAO
n1077		1990 Jul 11	4:56	-0.2	23.80	18 53 48.937	-21 59 13.20	13.9	1.3	11.4	Pal. KPNO CTIO Rio
n1078		1990 Jul 20	8:15	-1.0	22.96	18 52 46.529	-22 0 42.40	13.6	0.7	12.0	M.K. Pal. KPNO CTIO AAO
n1079		1990 Jul 28	0:33	-1.2	21.82	18 51 56.469	-22 1 54.58	13.8	1.0	11.8	CTIO Rio Ten. Pic. SAAO
n1080		1990 Aug 28	22:52	0.4	12.03	18 49 15.766	-22 6 2.35	13.7	1.1	11.6	Rio Ten. Pic. SAAO

• Declinations from two plates differ by 0.9"; average position given.

Observatory codes:
M.K. = Mauna Kea, Pal. = Palomar, KPNO = Kitt Peak, CTIO = Cerro Tololo, Rio = Rio de Janiero, Ten. = Teneriffe, Pic. = Pic du Midi, SAAO = Sutherland, Kav. = Kavalur, PMO = Purple Mtn. Obs., AAO = Anglo-Australian Obs..

struct the occultation geometry.

(ii) A maximum estimated K magnitude of 12.0 for Uranus and 13.0 for Neptune, based on the measured R and I magnitudes and our adopted calibration (see below). Experience has demonstrated that stars fainter than $K \simeq 12$ are unlikely to provide occultation data of sufficient quality for accurate Uranian-ring event timings. The fainter limit for Neptune stars is based on the brightness of the planet itself (variable, but often fainter than $K = 12$) and on the urgent need for further arc observations. Exceptions to these limits were made for a few Uranus stars from the list of Mink and Klemola (1985), which were estimated to fall below $K = 12.0$.

The apparent radius of the Earth, which determines the maximum local correction to the tabulated geocentric close-approach distances, is 0.49″ as seen from Uranus, and 0.30″ as seen from Neptune. Corresponding local corrections to the predicted close-approach times are $\lesssim 10$ min. Such corrections are no greater than likely errors in the predicted geocentric circumstances, and are thus not warranted at the present time.

In order for a particular event to be listed as observable at a certain station, the elevation of the planet at the predicted close-approach time was required to be at least 15°, while the Sun was required to be at least 10° below the horizon. These constraints may be unnecessarily strict in some cases, as they may eliminate slow (i.e., small v_{sky}) events for which at least a portion of the occultation may in fact be observable. Within a few months of conjunction (November to February, roughly), most of the predicted events are only observable in daylight or twilight. Particularly bright stars may still yield usable infrared data, even under these conditions, and their domains of observability may be approximately determined from the close-approach times listed in the tables and the planetary-transit times given in the *Astronomical Almanac*. We have retained all Neptune events during this period in Table II, regardless of night-time observability, but have omitted from Table I most of the Uranus events that occur while the planet is within 30° of the Sun. (A few exceptions were made for stars brighter than $K = 10.0$.)

Parameters for events identified from more than one plate pair have been averaged together in the tables. No significant positional or magnitude discrepancies were noted for such stars. Events previously identified by Mink and Klemola (1985) are so indicated in Tables I and II, using these authors' identification numbers. For completeness, we have also included in the tables Mink and Klemola stars that we did not recover; these stars are *not* assigned numbers in our system.

IV. PHOTOMETRIC CALIBRATIONS

a) R and I Magnitudes

As mentioned above, the 'magnitudes' obtained from the APM machine were expected to conform closely to a linear scale, but to have a poorly determined zero point for each plate. A comparison of the measured magnitudes for stars falling in the overlap regions of two plate pairs confirmed the existence of zero-point errors: mean magnitude offsets (R or

I) between a pair of plates were found to range from 0.4 to 1.8 mag. It was noted, however, that the mean $R-I$ color differences were much smaller, averaging only 0.3 mag.

We therefore adopted the following two-step procedure in calibrating the measured R and I magnitudes. First, all measured (or 'machine') magnitudes were reduced to a common system, based on one of the Uranus plates. The transformation between any particular plate and the standard plate was based on a linear fit to the measured differences between the two plates, δR vs R or δI vs I, obtained from the overlap region. The choice of a standard plate was based on a comparison of the scatter in the magnitude differences for various plate pairs, and on information on the quality of the original machine photometry. Because one of our plate pairs was used for both Uranus and Neptune searches, it was possible to put both sets of stars on a common magnitude scale.

In the second step, we utilized CCD photometry published by French *et al.* (1986) for Uranus occultation candidates from the list of Mink and Klemola (1985). These authors provide V_J and I_J magnitudes for 16 Uranus stars, on the Johnson system. The effective wavelength for I_J is 9000 Å, as compared with 8000 Å for the plate-derived I magnitude. The latter more closely approximates I on the Cousins photoelectric system (denoted I_C). Based on mean colors for main-sequence stars and giants on the Johnson and Cousins systems provided by Johnson (1966) and Cousins (1978), and intersystem transformations given by Bessel (1979), we obtain

$$I_C - I_J \simeq 0.22(V-I)_J$$
$$\simeq 0.29(V_J - I_C).$$

A comparison of our Uranus catalog with the data of French *et al.* (1986) reveals 11 stars in common, with a mean $(V-I)_J$ of 1.36 mag. The corresponding mean expected $I_C - I_J$ is ~ 0.30 mag, while our adjusted machine magnitudes give $\langle I_{\rm mach} - I_J \rangle = 1.86 \pm 0.08$ mag for the 11 stars. We have thus applied a uniform correction of -1.6 mag to the adjusted machine I magnitudes, in order to correct them at least approximately to the Cousins photoelectric system. We denote the corrected machine magnitudes by $I_{\rm plate}$. The resulting corrected magnitude differences $I_{\rm plate} - I_J$ are plotted vs $R-I$ in Fig. 1. The expected mean $R-I$ color for these 11 stars is ~ 0.50 mag, based on their mean $(V-I)_J$ and again using data provided by Bessel (1979). This is remarkably close to the mean $R-I$ of 0.64 ± 0.08 mag obtained directly from the adjusted machine magnitudes, especially considering the high and variable reddening in these fields. We have therefore elected to leave the machine-derived $R-I$ colors unchanged. We note that there is no obvious variation of $I_{\rm plate} - I_J$ with $R-I$, although the scatter in Fig. 1 is more than sufficient to disguise the expected small positive correlation. Tables I and II list $I_{\rm plate}$ and the uncorrected $R-I$.

Although the I magnitudes and $R-I$ colors in Tables I and II possess the virtue of being based directly on measurements from the plates, it would be more useful to know the K magnitudes of these stars. In principle, it is possible to estimate K from I and $R-I$, but there are two problems. Firstly, the leverage on the intrinsic stellar colors provided by $R-I$ is not great. The mean intrinsic color ratio for late-type giants and main-sequence stars is

$$I_C - K \simeq 2.5\ (R-I)_C.$$

Secondly, the degree of interstellar reddening exhibited by individual stars identified in this study is unknown, but is likely to be substantial in many cases. The reddening ratio obtained from the standard van de Hulst extinction law (Johnson 1968) is

$$I_C - K \simeq 2.04\ (R-I)_C.$$

The similarity of these two relations suggests that, on average, $I_C - K \simeq 2.3\ (R-I)_C$. However, given possible systematic errors of 0.2–0.3 mag in $R-I$, and a typical $R-I$ of ~ 1 mag, errors of as much as 1 mag in the predicted K are quite possible with this approach. We therefore prefer to use an independent empirical calibration of $I_{\rm plate} - K$ vs $R-I$ based on infrared photometry we have obtained for a subset of the Neptune stars in Table II.

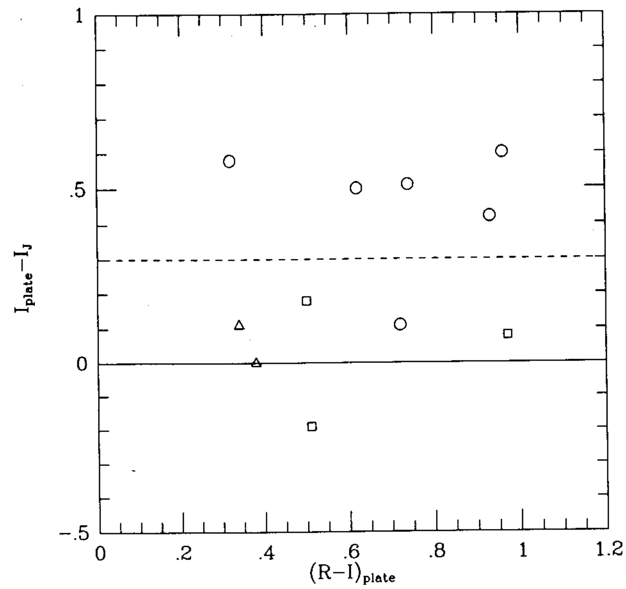

FIG. 1. Plate-derived I magnitudes for Uranus occultation candidates ($I_{\rm plate}$) compared with CCD measurements by French *et al.* (1986) (I_J). The raw APM magnitudes have been corrected by -1.6 mag in order to best match the CCD data, taking into account the expected mean $I_{\rm plate} - I_J$ color of 0.30 (see the text). Different symbols denote measurements made from different (R, I) plate pairs.

b) JHK Photometry

In Table III, we present *JHK* photometry for 67 of the 80 Neptune occultation candidates listed in Table II, plus seven of the eight Neptune stars from the list of Mink and Klemola (1985) not recovered in our search. The observations were made by one of us (Buie) during three nights on Mauna Kea: UT 1987 April 3 at the U.K. Infrared Telescope (UKIRT), and UT 1987 April 20 and UT 1987 May 23 at the NASA Infrared Telescope Facility (IRTF). The error bars reported represent one standard deviation in the photometric reductions, as discussed below.

On all nights, the pointing was checked against a few known stars in the same portion of the sky as the occultation candidates. As a result, it was possible to rely on the blind pointing of the telescope at the level of $\sim 1''$. All program stars were successfully located within $\sim 1''$ of the positions listed in Table II, although severe crowding resulted in a few instances of some uncertainty as to the identification of the correct star. In all such cases, the brightest infrared source within $1''$ of the tabulated position was measured. A few stars on the list could not be measured, either because of

TABLE III. *JHK* photometry of Neptune occultation candidates. Stars are identified by their numbers in Table II, and/or by the numbers assigned by Mink and Klemola (1985). A code indicates the night on which the observations were made (see Notes). The last three columns give photometric data from Covault and French (1986) and French *et al.* (1985).

Star	K	+-	J-H	+-	H-K	+-		M&K	K	J-H	H-K
n1001			not measured								
n1002			not measured								
n1003	11.52	0.02	0.74	0.02	0.13	0.03	1	N41	11.3	0.9	0.1
*	11.30	0.00	0.56	0.07	0.27	0.04	2				
n1004	11.78	0.01	0.44	0.03	0.04	0.03	1	N42	too dim		
	11.94	0.13	0.23	0.03	-0.21	0.15	1	N43	13.8		
n1005	7.66	0.01	0.64	0.02	0.16	0.02	1				
n1006	10.10	0.01	0.94	0.02	0.18	0.02	1				
n1007			confused field								
n1008	11.32	0.01	0.67	0.02	0.16	0.02	1				
*	11.01	0.01	0.61	0.06	0.24	0.04	2				
n1009	11.46	0.02	0.48	0.03	0.12	0.04	1	N44	11.3	0.3	0.2
n1010	10.66	0.01	0.81	0.02	0.24	0.02	1				
n1011	8.44	0.01	0.95	0.02	0.35	0.02	1				
	11.68	0.02	0.44	0.04	0.24	0.04	1	N45	11.1	0.7	0.1
n1012	10.35	0.01	0.95	0.02	0.23	0.02	1				
*	10.30	0.01	1.02	0.09	0.15	0.04	2				
n1013	9.72	0.00	0.89	0.04	0.38	0.02	2				
n1014	11.77	0.02	0.69	0.04	0.16	0.04	1				
n1015	10.81	0.00	0.23	0.04	0.14	0.02	2				
n1016	12.15	0.00	0.26	0.04	0.18	0.02	2				
n1017	10.75	0.00	0.64	0.04	0.24	0.02	2				
n1018	6.78	0.00	1.00	0.04	0.42	0.02	2				
n1019	10.40	0.00	0.69	0.04	0.25	0.02	2				
n1020	9.04	0.00	0.74	0.04	0.31	0.02	2				
n1021	13.37	0.06					1				
n1022	11.88	0.02	0.70	0.04	0.27	0.04	3				
n1023	12.76	0.03	0.38	0.05	0.20	0.06	3				
n1024	11.39	0.02	0.61	0.04	0.25	0.04	3				
n1025	8.97	0.00	0.85	0.04	0.33	0.02	2				
n1026	11.57	0.03	0.33	0.06	0.22	0.06	3	N46	9.0	1.3	0.4
n1027	9.81	0.01	0.64	0.02	0.20	0.02	1	N47	10.3	0.4	0.4
n1028	11.60	0.02	0.68	0.02	0.19	0.03	1				
n1029	11.97	0.01	0.70	0.02	0.18	0.02	1				
n1030			confused field								
n1031	10.43	0.01	0.62	0.02	0.12	0.02	1	N48	13.1		
n1032			confused field								
n1033			confused field								
n1034	11.40	0.00	0.56	0.03	0.21	0.02	2				
n1035	11.52	0.01	0.80	0.05	0.29	0.03	2				
	11.91	0.01	0.29	0.02	0.12	0.02	1	N49	too dim		
*	11.90	0.01	0.21	0.05	0.13	0.04	2				
n1036	11.65	0.02	0.32	0.02	0.02	0.03	1				
n1037	8.36	0.01	0.96	0.02	0.30	0.02	1				
	11.12	0.01	0.57	0.02	0.17	0.02	1	N50	too dim		
n1038	10.13	0.01	0.89	0.02	0.26	0.02	1				
n1039	10.42	0.00	0.75	0.05	0.31	0.03	2				
n1040	6.91	0.01	0.99	0.02	0.39	0.02	1	N51	too dim		
n1041	10.23	0.00	0.78	0.03	0.32	0.02	2				
n1042	10.90	0.01	0.25	0.05	0.15	0.05	1	N52	14.9		
n1043	9.67	0.01	0.67	0.02	0.21	0.02	1				

572

TABLE III. (continued)

Star	K	+-	J-H	+-	H-K	+-		M&K	K	J-H	H-K
n1044	8.76	0.02	1.00	0.04	0.42	0.04	3				
n1045	9.76	0.02	0.90	0.04	0.37	0.04	3				
n1046	10.95	0.02	0.80	0.04	0.30	0.04	3				
n1047	7.63	0.02	0.63	0.04	0.25	0.04	3				
n1048	9.36	0.02	0.62	0.04	0.26	0.04	3				
n1049	10.94	0.02	0.64	0.04	0.28	0.04	3				
n1050	11.94	0.02	0.78	0.04	0.30	0.04	3				
n1051	confused field										
n1052	not measured										
n1053	11.20	0.02	0.69	0.04	0.28	0.04	3				
n1054	8.17	0.02	1.01	0.04	0.37	0.04	3				
n1055	10.26	0.02	0.69	0.04	0.27	0.04	3				
n1056	11.41	0.02	0.73	0.04	0.25	0.04	3				
n1057	12.08	0.02	0.22	0.04	0.19	0.04	3				
n1058	source in reference beam										
n1059	11.84	0.02	0.64	0.05	0.23	0.05	3				
n1060	12.80	0.03	0.39	0.06	0.18	0.06	3				
n1061	11.13	0.02	0.41	0.04	0.23	0.04	3	N53	11.3	0.5	0.2
n1062	12.32	0.02	0.72	0.04	0.25	0.04	3				
n1063	7.22	0.02	1.00	0.04	0.44	0.04	3				
n1064	12.65	0.04	0.36	0.05	0.18	0.07	3				
	12.55	0.02	0.27	0.04	0.19	0.04	3	N54	12.3	0.3	0.4
n1065	11.99	0.02	0.68	0.04	0.28	0.04	3				
n1066	11.64	0.02	0.71	0.04	0.22	0.04	3				
	5.43	0.02	1.00	0.04	0.43	0.04	3	N55	5.5	1.0	0.4
n1067	source in reference beam										
n1068	12.96	0.03			0.21	0.11	3				
n1069	12.13	0.03	0.53	0.04	0.26	0.05	3				
n1070	confused field										
n1071	source in reference beam										
n1072	11.60	0.03	0.66	0.06	0.28	0.06	3				
n1073	11.87	0.03	0.33	0.06	0.20	0.06	3				
n1074	10.42	0.04	0.29	0.08	0.24	0.08	3				
n1075	10.43	0.04	0.68	0.08	0.35	0.08	3				
	9.21	0.03	0.14	0.06	0.19	0.06	3	N57	9.5	0.2	0.0
n1076	12.54	0.04	0.49	0.06	0.28	0.07	3				
n1077	11.39	0.03	0.70	0.06	0.31	0.06	3				
n1078	11.53	0.03	0.74	0.06	0.31	0.06	3				
n1079	12.40	0.04	0.41	0.08	0.23	0.08	3				
n1080	source in reference beam										
	6.38	0.01	0.74	0.05	0.49	0.04	2	N99			

Notes:

1 = UKIRT observations, 3 April 1987.
2 = IRTF observations, 20 April 1987.
3 = IRTF observations, 23 May 1987.
* duplicate observation of same star

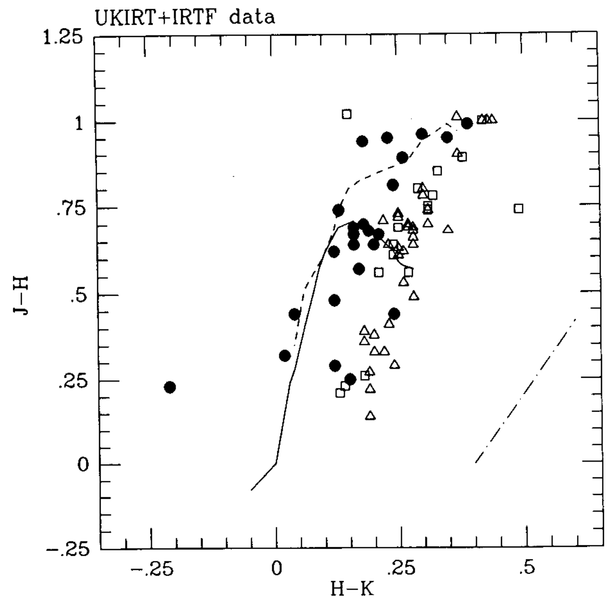

FIG. 2. $J-H$ vs $H-K$ colors for Neptune occultation candidates. Dark circles indicate UKIRT measurements on 3 April, while squares and triangles indicate IRTF measurements on 20 April and 23 May, respectively. No attempt has been made to put these two data sets on a common photometric system, and some systematic color differences are apparent at the 0.1–0.2 mag level (see the text). The solid line shows the intrinsic relation for main-sequence stars, and the dashed line that for late-type giants (Lee 1970). The reddening relation of Jones and Hyland (1980) is indicated by the dot-dashed line.

excessive confusion or because there was a bright star in the reference beam. In all such cases, however, there was at least one source brighter than $K=12$ present near the tabulated position.

The photometric reduction on the nights of April 3 and April 20 was straightforward and followed standard procedures. No attempt has been made here to correct for any systematic differences between the UKIRT and IRTF photometers. Inspection of the four measurements that overlap between the two telescopes reveals a systematic shift of $J_{\mathrm{UKIRT}}-J_{\mathrm{IRTF}}=0.17\pm0.06$, $H_{\mathrm{UKIRT}}-H_{\mathrm{IRTF}}=0.11\pm0.05$, and $K_{\mathrm{UKIRT}}-K_{\mathrm{IRTF}}=0.15\pm0.07$. However, the photometry presented here should suffice for the present purpose of selecting suitable events for observations. The reduction on the night of May 23 was complicated by ruined standard-star measurements. As a result, the extinction could be determined only from back-to-back measurements of each of the two standard stars. No meaningful error bars on the extinction could be determined, and an arbitrary uncertainty of ±0.1 mag/airmass was assigned. For all stars measured on this night, the extinction error bar dominates the uncertainty in the photometry.

Figure 2 is a two-color diagram for the measured Neptune candidates, comparing our measured colors with the intrinsic colors for main-sequence and giant stars. The latter are taken from Lee (1970), while the galactic reddening line is from Jones and Hyland (1980). In general, the observed colors are consistent with the moderately reddened late-type giants expected to dominate the stellar population in the galactic plane (Elias 1978), although there appears to be a systematic difference amounting to $\sim$0.1–0.2 mag in $H-K$ between the UKIRT and IRTF measurements. This difference is probably due to variations in the filter transmissions and/or detector-response functions between the two photometers, but we have not investigated it further.

The resulting $I_{\mathrm{plate}}-K$ colors are plotted vs $R-I$ in Fig. 3 (the plate-derived I magnitudes have been corrected by -1.6 mag, as discussed above). A linear fit to these data yields the relation

$$I_{\mathrm{plate}}-K=0.58+1.47\times(R-I)_{\mathrm{plate}},$$

which is somewhat flatter than the expected relation. We note that the smallness of the zero-point term in the fitted relation provides additional confidence in the approximate correctness of the $R-I$ colors derived from the machine magnitudes, and in the -1.6 mag correction applied above to the I magnitudes. This empirical linear relation is used to estimate K magnitudes (K_{est}) for all of the candidate stars in Tables I and II.

The rms scatter of 0.6 mag about the linear fit is somewhat greater than that in Fig. 1, as might be expected. The relation between K magnitudes and $R-I$ colors will be unavoidably uncertain at this Galactic latitude. The reddening is large and highly variable on small angular scales, so that the intrinsic stellar locus in the $R-I/I-K$ plane is likely to provide only a general indication of the true distribution of these stars. Nevertheless, the data in Fig. 3, together with results obtained from previous occultations in 1984–1986, indicate that such an empirical relation provides a reasonably satisfactory basis for the estimation of K magnitudes from R and I magnitudes.

c) Comparison with Previous Photometry

Covault and French (1986) have also published *JHK* photometry for Uranus and Neptune occultation candi-

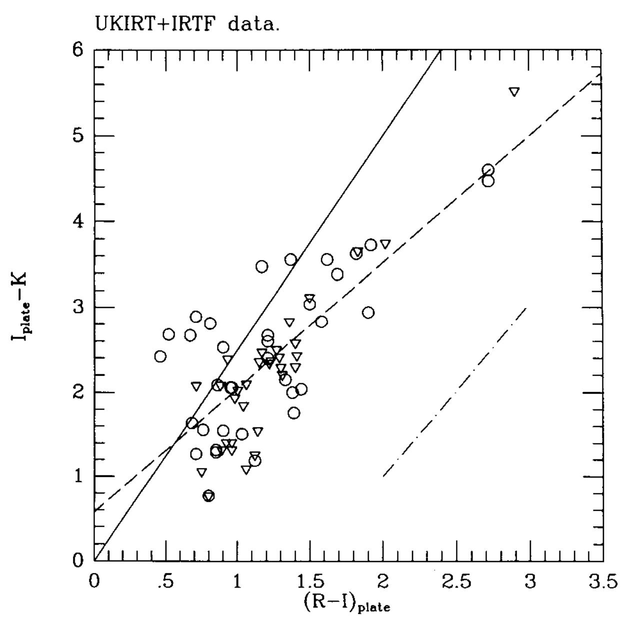

FIG. 3. $I-K$ for Neptune occultation candidates vs $R-I$ colors derived from plate scans. The individual observed K magnitudes are given in Table III. Different symbols denote stars measured from different (R, I) plate pairs. The best-fitting linear relation, $I_{\mathrm{plate}}-K=0.58+1.47\times(R-I)$, shown as a dashed line, is used to estimate the K magnitudes in Tables I and II from I and $R-I$. The solid line with a slope of 2.5 represents the intrinsic locus for late-type stars (Cousins 1978), while the standard van de Hulst reddening relation is shown by the dot-dashed line.

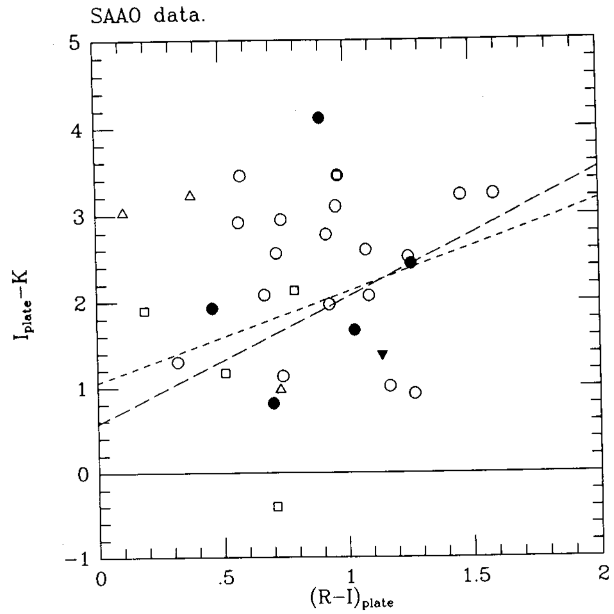

FIG. 4. $I-K$ for Uranus and Neptune occultation candidates vs $R-I$ colors derived from plate scans. The measured K magnitudes are from Covault and French (1986). Different symbols denote stars measured on different (R, I) plate pairs, with light and dark symbols representing Uranus and Neptune stars, respectively. The short-dashed line is a least-squares fit to these data: $(I-K) = 1.06 + 1.05\times(R-I)$, which is not appreciably different from the linear fit to the UKIRT/IRTF data from Fig. 3, shown by the long-dashed line. Note the large scatter of the data about either fit.

dates, based on measurements at the 30 and 74 in. telescopes at the South African Astronomical Observatory (SAAO). A comparison of their data with Tables I and II reveals 32 stars in common, mostly Uranus candidates, and the corresponding $I_{\text{plate}} - K$ colors are plotted vs $R-I$ in Fig. 4. This plot reveals a rather scattered distribution of points, with almost no correlation between $I-K$ and $R-I$. These data, however, cover a smaller range of $R-I$ than do those in Fig. 3, and this may contribute to the apparent lack of correlation. A linear least-squares fit to these data, while not well constrained, is not significantly different from that obtained from the UKIRT/IRTF data (see Fig. 4). The rms residuals of the SAAO measurements, however, are ~ 1.4 mag, much larger than those of the present observations.

The SAAO observations were made with 18″ diameter apertures (Covault and French 1986), whereas the UKIRT/IRTF observations employed aperture diameters of 12.4″. This suggests that some of the SAAO K measurements may have been contaminated by strongly reddened background stars, which are extremely abundant in this region of the sky. Several examples of such confusion were noted during our own observations (see the Notes to Table III), including instances of background sources appearing in both measurement and sky reference beams.

In the last three columns of Table III we give the K magnitudes and infrared colors measured for Neptune candidates by Covault and French (1986), together with some additional data from French *et al.* (1985). In eight out of nine cases, the photometry of Covault and French is in agreement with the present results to within ± 0.6 mag. The exception is star N46, which we find to be 2.6 mag fainter at $K = 11.6$. Seven additional Neptune candidates listed by Mink and Klemola (1985) were reported by Covault and French to be either fainter than $K = 13$ or to be too dim to measure. Our observations, however, indicate that all seven stars are in fact brighter than $K = 12$, with N51 being the third brightest (at $K = 6.9$) of the 75 stars measured. We have been unable to resolve these inconsistencies, but suspect that the problem may lie in contamination of either measurement or reference beams by optically faint infrared sources, and perhaps in a few instances of source misidentification. Whatever the explanation of the discrepancies, this situation points up the need for extreme care in obtaining reliable infrared photometry of occultation candidates for Uranus and Neptune.

V. DISCUSSION

The lists of occultation candidates presented in Tables I and II supplement those published by Mink and Klemola (1985), but differ in emphasizing the late-type and reddened stars, which are the most suitable for infrared observations. Of the 43 Uranus candidates identified over this time period by Mink and Klemola (1985), 35 have been recovered in the present survey. For Neptune, the recovery rate is a somewhat lower ten out of 17. No obvious relationship exists between the V magnitudes of the stars and their chances of recovery. No significant positional discrepancies were noted for any of the 45 recovered stars.

In addition, a considerable number of new occultation candidates have been identified, many of which are either measured or predicted to be as bright at λ 2.2 μm as the brightest of Mink and Klemola's stars. This result, together with our previous test investigation, amply demonstrates the value of near-infrared searches for outer-planet occultation candidates. Even more effective would be a specialized λ 2.2 μm imaging survey of the regions traversed by the planets. Such a survey, carried to a modest limiting magnitude of $K = 13$, say, would be quite feasible with currently available infrared-imaging systems and a telescope with reliable computer-controlled pointing.

We draw particular attention to the following events, involving unusually bright stars and relatively small close-approach distances:

Uranus: u1056 and u1059 in 1988; u1078 ($K_{\text{est}} = 6.9$, also visible in daylight at Ten., Pic, SAAO), u1087 (also visible in daylight at Pal., KPNO, CTIO), u1093 and u1115 (also visible in daylight at Rio, Ten., Pic, SAAO) in 1989; and u1157 in 1990 ($K_{\text{est}} = 7.5$, visible in daylight at AAO, M.K., Pal.). Also of special interest are events U61 (= u1133), U65 (= u1136), U70 (= u1146), and U73 (= u1149) of Mink and Klemola (1985), all occurring in 1990.

Neptune: n1018 in December 1987 ($K = 6.8$, visible in daylight at PMO, AAO, M.K.); n1025 (also visible in daylight at PMO, AAO), n1027 (= N47), n1031 (= N48), n1037, n1040 (= N51, also visible in daylight at Rio, CTIO) and n1047 ($K = 7.6$, visible in daylight at PMO, AAO, M.K.) in 1988; and n1063 in 1989 (also visible in daylight at Kav.).

In addition to the above, events u1086, u1108, u1152, n1040, and n1069 occur close to a stationary point on the planet's trajectory, and thus exhibit unusually low sky-plane velocities. The signal-to-noise ratio for data obtained for such events can be improved markedly by increasing the integration time, without unduly sacrificing resolution.

Detailed predictions for any of the events listed in Tables I and II calculated for specific observatories are available on request from P. D. Nicholson, as are computer-generated finding charts based on the Schmidt-plate scans.

We should like to thank D. Mink and A. Klemola for providing their extensive catalog of unpublished stellar positions, and M. Standish for the provision of planetary ephemerides. L. French kindly provided photometric data in advance of their publication. D. Tholen and K. Kristunis assisted with the photometric observations. M. Buie acknowledges the support of the United Kingdom Infrared Telescope, which is operated by the Royal Observatory Edinburgh on behalf of the U. K. Science and Engineering Research Council. This work was funded in part by JPL Contract LN-766489, in support of *Voyager* mission planning. Additional support was provided by NASA grants NAGW-544 and NGL 12-001-057.

REFERENCES

Bessel, M. S. (1979). Dudley Obs. Rep. No. 14, 279.

Cooke, M. L., Nicholson, P. D., Matthews, K., and Elias. J. (1985). Bull. Am. Astron. Soc. **17**, 719.

Cousins, A. W. J. (1978). Mon. Not. Astron. Soc. S. Afr. **37**, 62.

Cousins, A. W. J. (1980). Mon. Not. Astron. Soc. S. Afr. **39**, 22.

Covault, C. E., and French, L. M. (1986). Icarus **66**, 630.

Covault, C. E., Glass, I. S., French, R. G., and Elliot, J. L. (1986). Icarus **67**, 126.

Elias, J. H. (1978). Astrophys. J. **223**, 859.

Elliot, J. L., Dunham, E. W., and Mink, D. J. (1977). Nature **267**, 328.

Elliot, J. L., and Nicholson, P. D. (1984). In *Planetary Rings*, edited by A. Brahic and R. Greenberg (University of Arizona, Tucson).

Fink, U., and Larson, H. P. (1979). Astrophys. J. **233**, 1021.

French, L. M., Covault, C. E., Morales, G. M., Gaiser, S. L., and Frogel, J. (1985). Bull. Am. Astron. Soc. **17**, 700.

French, L. M., Morales, G., Gaiser, S. L., and Frogel, J. A. (1986). Icarus **67**, 540.

French, R. G., Elliot, J. L., French, L. M., Kangas, J. A., Meech, K. J., Ressler, M., Buie, M. W., Frogel, J. A., Holberg, J. B., Jimenez-Fuensalida, J., Joy, M., and Simpson, R. A. (1987). Icarus (submitted).

Gilmore, G. (1984). In *Astronomy with Schmidt-Type Telescopes*, edited by M. Capaccioli (Reidel, Dordrecht), p. 77.

Goldreich, P., and Tremaine, S. (1982). Annu. Rev. Astron. Astrophys. **20**, 249.

Guinan, E. F., Harris, C. C., and Maloney, F. P. (1982). Bull. Am. Astron. Soc. **14**, 658.

Hubbard, W. B. (1986). Science **231**, 1276.

Hubbard, W. B., Brahic, A., Sicardy, B., Elicer, L. R., Roques, F., and Vilas, F. (1986). Nature **319**, 636.

Hubbard, W. B., Nicholson, P. D., Lellouch, E., Sicardy, B., Brahic, A., Vilas, F., Bouchet, P., McLaren, R. A., Millis, M. L., Wasserman, L., Elias, J. H., Matthews, K., McGill, J. D., and Perrier, C. (1987). Icarus (in press).

Johnson, H. L. (1966). Annu. Rev. Astron. Astrophys. **4**, 193.

Johnson, H. L. (1968). In *Stars and Stellar Systems*, Vol. VII, edited by L. H. Aller and B. M. Middlehurst (University of Chicago, Chicago).

Jones, T. J., and Hyland, A. R. (1980). Mon. Not. R. Astron. Soc. **192**, 359.

Klemola, A. R., Mink, D. J., and Elliot, J. L. (1981). Astron. J. **86**, 138.

Lee, T. E. (1970). Astrophys. J. **162**, 217.

Lellouch, E., Hubbard, W. B., Sicardy, B., Vilas, F., and Bouchet, P. (1986). Nature **324**, 227.

Mink, D. J., and Klemola, A. (1985). Astron. J. **90**, 1894.

Mink, D. J., Klemola, A. R., and Elliot, J. L. (1981). Astron. J. **86**, 135.

Nicholson, P. D., Cooke, M. L., Matthews, K., Elias, J., and Gilmore, G. (1988). In preparation.

Reid, N., and Gilmore, G. (1982). Mon. Not. R. Astron. Soc. **201**, 73.

Sicardy, B., Bouchet, P., Brahic, A., McLaren, R., Perrier, C., and Roques, F. (1985). Bull. Am. Astron. Soc. **17**, 923.